Deviations from $T^{3/2}$ Law for Magnetization of Ferrometals: Ni, Fe, and Fe+3% Si

B. E. ARGYLE, S. H. CHARAP, AND E. W. PUGH*
International Business Machines Corporation, Yorktown Heights, New York
(Received 26 July 1963)

The variation with temperature of the magnetizations of single crystals of Ni, Fe, and Fe+3 wt % Si are studied. New data for Fe and Fe(Si) is presented along with previously reported measurements for Ni. These data were obtained by means of the pyromagnetic effect at various applied fields and in the temperature range 4.2–140, 30, and 120°K for the Fe, Fe(Si), and Ni crystals, respectively. The observed departures from $T^{3/2}$ behavior are well described by spin-wave theory. Attempts to ascribe some of the measured variation of the magnetization to Stoner-type excitations or to variation of the moment per atom due to lattice expansion are mainly unsuccessful. The coefficients of the $T^{3/2}$ term appropriate for zero spin-wave energy gap are $C=7.5\pm0.2$, 3.4 ± 0.2, and $4.4\pm0.2\times10^{-6}$ deg$^{-3/2}$ for Ni, Fe, and Fe(Si), respectively. The coefficients of the $T^{5/2}$ term for zero gap are determined only for the Ni and Fe crystals as $D=(1.5\pm0.2)\times10^{-8}$ deg$^{-5/2}$ and $(1\pm1)\times10^{-9}$ deg$^{-5/2}$, respectively. The measured variation of the spin-wave energy gap with applied field is consistent with the known g values of 2.19 and 2.09 for Ni and Fe. The magnitude of the gap at zero field is fully explained by the effects of magnetocrystalline anisotropy and magnetic-dipolar coupling. The values of the C and D coefficients are compared with results from independent experiments and are discussed in relation to theories of ferromagnetism in metals.

IN recent years it has been established that spin-wave excitations exist in metals and that they provide the dominant mechanism for initial decay of the ferromagnetic moment. This is an important step toward the ultimate understanding of ferromagnetism in metals. Spin-wave resonance[1–3] and inelastic neutron scattering studies[4,5] can both provide the spin-wave dispersion relation and its $T^{5/2}$ temperature dependence resulting from spin-wave–spin-wave interactions. On the other hand, the best evidence for the dominance of spin-wave phenomena in determining the temperature dependence of the magnetization has been supplied by pyromagnetic observations.[6–8] While these measurements are not able to detect spin-wave–spin-wave interactions, they do reveal clearly details of the spin-wave dispersion curve not previously studied experimentally, such as the total energy gap and the quartic dependence on wave vector.

Recent improvements in the method of analyzing these data make it possible to separate from the dominant spin-wave result the higher order effects which are not predicted by simple spin-wave theory. With these improvements, it has been found necessary to revise some of the details of our previous work[8] on nickel. We also present here new measurements on Fe and Fe+3 wt % Si. In the data analysis of all three materials, deviations from the $T^{3/2}$ form which are predicted by spin-wave theory are separated from other effects such as Stoner-type excitations and lattice expansion, and an attempt is made to determine which of these is dominant.

Previous experimental work in this field includes that by Fallot[9] and by Foner and Thompson.[10] The accuracy of Fallot's measurements of total magnetization versus temperature on polycrystalline Fe and Ni was just sufficient to permit making a distinction between a $T^{3/2}$ and a T^2 law. Foner and Thompson reported a nearly $T^{3/2}$ behavior in their single crystal of Ni, no effect of applied field and an anomalous minimum in the M versus T curve near 10°K. In contrast, the pyromagnetic method is sensitive enough to measure in detail the effects of an applied field but has given no evidence of an anomalous minimum.[11]

In Sec. I, the pyromagnetic method is reviewed. The earlier data on Ni along with new data on crystals of Fe and Fe+3% Si is presented with particular attention given to the variation of data accuracy as a function of temperature. In Sec. II, we discuss the theoretical equation used for analysis of the magnetization temperature dependence. Data analysis by the least-squares method is outlined in Sec. III with special emphasis given to the removal of ambiguities peculiar to this theoretical form with our present data accuracy. The results will be seen to indicate that deviations from a $T^{3/2}$ law are best described by a detailed spin-wave theory rather than effects associated with Stoner-type

* Present address: IBM Components Division, Poughkeepsie, New York.

[1] G. T. Rado and J. R. Weertman, Phys. Chem. Solids **11**, 315 (1959).

[2] M. H. Seavey, Jr., and P. E. Tannenwald, Suppl. J. Appl. Phys. **30**, 227S (1959).

[3] P. E. Tannenwald, J. Phys. Soc. Japan **17**, Suppl. B-1, 592 (1962).

[4] R. N. Sinclaire and B. N. Brockhouse, Phys. Rev. **120**, 1638 (1960).

[5] R. D. Lowde (private communication).

[6] E. W. Pugh and B. E. Argyle, Suppl. J. Appl. Phys. **32**, 334S (1961).

[7] B. E. Argyle and E. W. Pugh, Bull. Am. Phys. Soc. **6**, 125 (1962).

[8] E. W. Pugh and B. E. Argyle, Suppl. J. Appl. Phys. **33**, 1178 (1962).

[9] M. Fallot, Ann. Phys. (N. Y.) **6**, 305 (1936).

[10] S. Foner and E. D. Thompson, Suppl. J. Appl. Phys. **30**, 229S (1959).

[11] The large low-temperature anomaly is now thought to have been caused by spurious effects in the sample support mechanism: S. Foner (private communication).

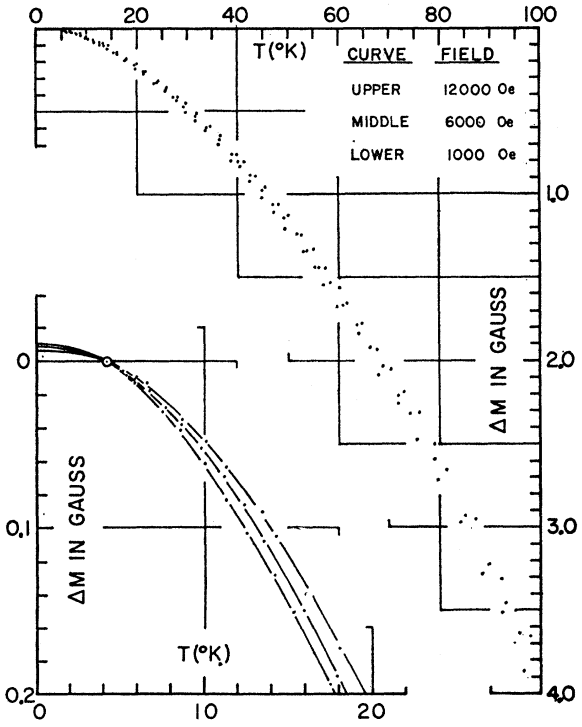

FIG. 1. Observed decreases in magnetization of a single crystal nickel sphere with temperature above 4.2°K($\triangle M=0$ at $T=4.2$°K). The fields indicated were applied parallel to the [111] crystal axis and have been corrected for demagnetizing effects so as to represent internal applied fields. The curves in the lower left corner are the low-temperature portions of the larger curves and are presented on an expanded scale.

excitations or lattice expansion. In other words, an adequate fit to our pyromagnetic data would be obtained were the terms characterized by the coefficients S and E in Eq. (1) completely neglected. Finally in Sec. IV are summarized the resulting best values or limits on fitting parameters. From these are inferred quantitive details of the spin-wave dispersion relation which are compared with results from spin-wave resonance, inelastic neutron scattering and ferromagnetic resonance measurements. The implications of these results for cubic ferromagnetic metals are reviewed in Sec. V.

I. PYROMAGNETIC DATA

The samples measured were single crystal spheres[12] of Ni, Fe, and Fe+3 wt.% Si having diameters 0.5, 0.325 and 0.55 in., respectively. The observed decreases in magnetization with temperature from the value at 4.2°K are presented in Figs. 1 and 2 and are seen to span a range of $\triangle M$ that never exceeds 1% of the total magnetization. The character of the data on the Ni and Fe+3% Si crystals is similar in that both show a discernable dependence of the magnetization curves on applied field. In the case of pure Fe a curve at only one applied field is shown, because the curves measured at different applied fields were not significantly different. This is due to its reduced size; larger sizes were not available to us because of the well-known difficulties of growing single crystals of pure iron. Nevertheless, data from this sample is useful not only because it represents the pure state of the element, but also because it was possible to maintain reasonable accuracy to considerably higher temperatures than was the case for the larger sized Fe(Si) sphere. It is well known that addition of 3 wt.% silicon serves to bypass the difficulty of growing large crystals and at the same time does not alter significantly the average magnetic moment per iron atom. The volume of Fe(Si) sphere is by design more than four times that of the sphere of pure Fe; this restores the sensitivity of data to changes in applied field as in Fig. 2. It also has 30% more volume than the sphere of Ni which further enhances sensitivity in order to overcome a smaller range of H ($\approx$7 kOe in contrast to 12 kOe) available above the demagnetizing field.

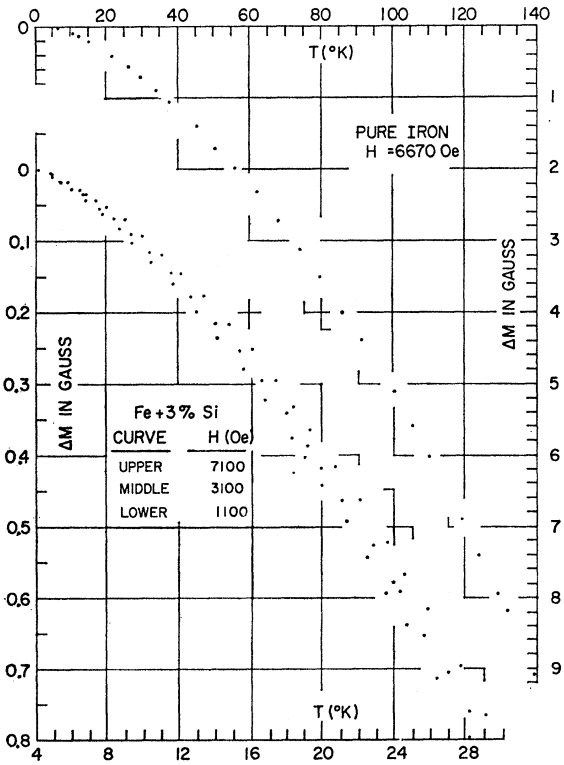

FIG. 2. Observed magnetization changes with temperature in single crystal iron. Upper curve was obtained from a small iron sphere (diam=0.325 in.) with the applied field parallel to [100]. Lower curves were measured on larger sphere of Fe+3% Si (diam=0.55 in.) with the field applied parallel to [110] and are presented on an expanded scale. The indicated applied fields have been corrected for demagnetizing effects ($\frac{4}{3}\pi M=7330$ Oe for pure iron and 6920 Oe for Fe+3% Si).

[12] The spheres were supplied by J. F. Kirn of the Virginia Institute for Scientific Research. Starting materials for the Fe and Ni crystals were 99.94% pure and for the alloy of Fe(Si) were 99.999% pure.

Details of the pyromagnetic technique have been discussed elsewhere.[8] Briefly, the method consists of detecting changes in magnetization of a sample when heated from 4.2°K to a new temperature in a fixed external field. The sample is spherical in shape and is aligned with a principal crystal axis parallel to a well-regulated constant field of magnitude sufficient to ensure that the magnetic state is that of a single domain. The temperature change is induced by passing current through carbon resistors attached to the sample and measured by a calibrated thermocouple soldered to the sample. Temperature uniformity at the peak of the temperature pulse is indicated by an approximate technique of noting the temperature difference between hot and cold points of the sample. By controlling the rate of heating, the maximum temperature difference is held to less than $\frac{1}{2}\%$ of the peak temperature which is read to within 0.1°K. Changes in sample flux are detected by a pair of Helmholtz coils, whose output is fed to a sensitive integrating circuit. The combined system is capable of detecting changes of 10^{-4} G in magnetization of a 0.5-in-diam sphere of nickel. In practice, the presence of background noise reduces this to 10^{-3} so that in Ni ($M_0=508$ G.) relative changes of 2 parts per million (ppm) are measurable, while in Fe ($M_0=1752$) changes of less than 1 ppm are measurable. This order of change is that expected for a one degree change in temperature. Because thermal expansion coefficients are also of the order of ppm per degree, special care was used to prevent inductive pickup of the applied field by the changes in coil dimensions. This was achieved by thermally anchoring the copper coil forms to 4.2°K. A Helmholtz geometry for the pickup coil was selected in order to minimize inductive coupling to the motion of the sample caused by its thermal expansion and that of its supports.

Figure 3 shows the approximate percent error in ΔM at all temperatures for all three samples as determined from background noise and estimated maximum consistent errors. Since the percent error is nearly constant over a wide range of temperature, the absolute error increases nearly in proportion to ΔM and, therefore, approximately with $T^{3/2}$. Thus, in the least-squares fitting procedure we now weight the data according to $T^{-3/2}$. This provides significant improvement over the analysis technique previously used on the nickel data.

Methods for estimating errors have been detailed by Pugh and Argyle.[8] The low-temperature region (up to 10°K) is dominated by errors obtained when measuring the background signal from paramagnetic impurities in carbon resistor heaters and Au+2.1 at.% Co thermocouple. The temperature region (10–20°K) is dominated by noise in the Helmholtz coil circuit due to voltage fluctuations induced thermally during the temperature pulse. In addition to some of this error, the region of the plateau contains a 1% readability error. Finally, a combination of errors unique to each sample becomes large enough to limit the final temperature. In the case

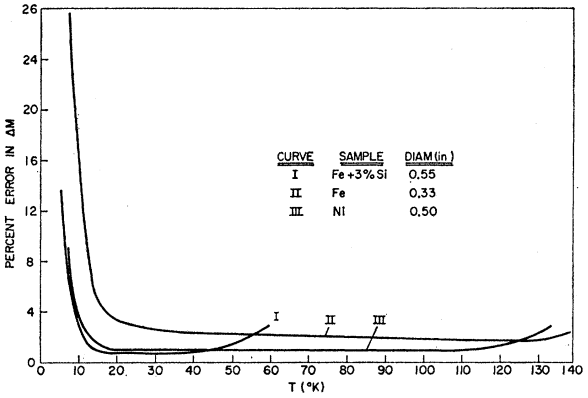

FIG. 3. Approximate percent error in measurements of change in magnetization from 4.2°K to each temperature T for the indicated single crystal spheres.

of Fe, for example, the thermal cycle became long enough (≈ 2 min.) compared to the time constant of the integrator (15 min.) that integrator drift contributed 2% error in ΔM at 140°K. This same consideration limited the maximum temperature for Fe(Si) to approximately 65°K. However, the requirement of temperature uniformity was not satisfied unless its final temperature was held down to 30°K.

II. THEORETICAL EQUATION

The following equation for the intrinsic domain magnetization M at a temperature T is expected to represent the behavior of a ferromagnetic metal:

$$\frac{M_0-M(T)}{M_0}=\beta\left(\frac{3}{2},\frac{T_g}{T}\right)CT^{3/2}+\beta\left(\frac{5}{2},\frac{T_g}{T}\right)DT^{5/2}+\cdots+ST^2+E\frac{\Delta l(T)}{l_0}. \quad (1)$$

Here M_0 is the value of M at $T=0$°K. The functions

$$\beta\left(\frac{3}{2},\frac{T_g}{T}\right)$$

and

$$\beta\left(\frac{5}{2},\frac{T_g}{T}\right)$$

which multiply the C and D coefficient reduce to unity if the applied and effective internal magnetic fields vanish. Inclusion of these fields produces a gap k_BT_g (k_B is Boltzmann's constant) in the spin-wave spectrum with resultant field and temperature dependence as discussed later in this section. The half-integer powers of T shown explicitly are an adequate description of spin-wave phenomena in the temperature range of this experiment,[13] the term in T^2 is considered to be the most

[13] We may depend entirely on experimental evidence in inelastic scattering of neutrons (see Ref. 5) and spin-wave resonance (see Ref. 3) for this statement. All that is required is that spin-wave energies have a predominantly quadratic dependence on wave vector which is largely independent of temperature.

appropriate description of collective electron behavior, and the last term is included to account for the possibility that the magnetic moment per atom may vary with lattice separation.

For a justification of the spin-wave terms it is not necessary to rely on the Heisenberg model; the spin-wave spectrum must have the full symmetry of the crystal and may, therefore, be expanded[14] as

$$\epsilon_{\mathbf{k}}=\epsilon_0-2S_j\sum_{\mathbf{l}}J_l\cos\mathbf{k}\cdot\mathbf{l}, \tag{2}$$

where the $\mathbf{l}$ are lattice vectors and we *may* call the coefficients J_l exchange integrals. A factor $2S_j$ has been included to provide contact with the Heisenberg model. The constant ϵ_0 is determined by the requirement that the $\mathbf{k}=0$ spin wave has no energy in the absence of magnetic effects and is

$$\epsilon_0=2S_j\sum_{\mathbf{l}}J_l. \tag{3}$$

It is useful and valid for small $\mathbf{k}$ to expand the energy (2) in powers of $\mathbf{k}\cdot\mathbf{l}$:

$$\epsilon_{\mathbf{k}}=\frac{2S_j}{6}k^2\sum_{\mathbf{l}}l^2J_l-\frac{2S_j}{24}\sum_{\mathbf{l}}(\mathbf{k}\cdot\mathbf{l})^4J_l+\cdots. \tag{4}$$

The quadratic term has been derived for a structureless "sea" of magnetic spin density by Herring and Kittel[15] and the remaining terms therefore describe the perturbing effect of the magnetic lattice. It should be noticed that the relative magnitudes of successive terms in (4) depend on the variation of J_l with distance.

The magnetization is obtained by associating with each spin wave a reduction of M_0/NS_m, which is just equal to $g\beta$.[15] Here g is the spectroscopic splitting factor, β the Bohr magneton, N the atomic density and S_m the spin per atom. By counting the spin waves according to the Bose-Einstein distribution over the energies given by Eq. (4), one obtains the result[16]

$$\frac{M_0-M(T)}{M_0}=\frac{2.612}{NS_m}\left\{\frac{3k_BT}{4\pi S_j\sum_{\mathbf{l}}l^2J_l}\right\}^{3/2}+\frac{1.341}{NS_m}\frac{3\pi}{4}\times\left(\frac{\sum_{\mathbf{l}}l^4J_l}{\sum_{\mathbf{l}}l^2J_l}\right)\left\{\frac{3k_BT}{4\pi S_j\sum_{\mathbf{l}}l^2J_l}\right\}^{5/2}+\cdots, \tag{5}$$

which specifies the coefficients C and D of Eq. (1). The experimental value of the ratio D/C yields information on the range of J_l which will be seen to extend beyond nearest neighbors.

The effects of an applied field, anisotropy, and spin-wave demagnetization can be combined and described by an energy gap ϵ_g in the spin-wave spectrum of Eq. (4). We define a gap temperature $T_g=\epsilon_g/k_B$ and find that Eq. (5) must be modified[8] by multiplying the $T^{3/2}$ term by the factor

$$\zeta\left(\frac{3}{2},\frac{T_g}{T}\right)=\frac{1}{2.612}\sum_{n=1}^{\infty}n^{-3/2}\exp\left[-\frac{nT_g}{T}\right] \tag{6a}$$

$$\approx\frac{1}{2.612}\left\{-3.54\left(\frac{T_g}{T}\right)^{1/2}+2.612+1.46\frac{T_g}{T}-0.104\left(\frac{T_g}{T}\right)^2+\cdots\right\}, \tag{6b}$$

and the $T^{5/2}$ term by the factor

$$\zeta\left(\frac{5}{2},\frac{T_g}{T}\right)=\frac{1}{1.341}\sum_{n=1}^{\infty}n^{-5/2}\exp\left[-n\frac{T_g}{T}\right] \tag{7a}$$

$$\approx\frac{1}{1.341}\left\{2.36\left(\frac{T_g}{T}\right)^{3/2}+1.341-2.61\frac{T_g}{T}-0.730\left(\frac{T_g}{T}\right)^2+\cdots\right\}. \tag{7b}$$

These factors reduce to unity when T_g vanishes since the sums then become the Riemann zeta functions $\zeta(\frac{3}{2})=2.612$ and $\zeta(\frac{5}{2})=1.341$. The defining series [Eqs. (6a) and (7a)] converge very slowly if $T\gg T_g$. For example, if $T_g/T\approx0.01$, it requires $\sim10^4$ terms to produce 1% accuracy. The second series [Eqs. (6b) and (7b)] apparently were first applied to energy gap effects by Charap.[17] They converge for $T_g/T\leq2\pi$ and the terms written here give 1% accuracy if $T_g/T\leq1$. It may be noted that the leading gap correction to Eq. (5) is linear in T, in agreement with a result first obtained by Holstein and Primakoff.[18] We have, however, used all necessary terms of each series in the least-squares analysis of data. The choice between the high- and low-temperature forms of the ζ functions was automatically made by means of a "switch" at $T=T_g$ that was incorporated into the IBM-7090 computer program.

To evaluate the energy gap we first use the fact that each spin-wave excited is associated with a reduction of $g\beta$ in the moment of the system and, therefore, with an energy $g\beta H$, where H is the total internal magnetic field (external minus demagnetization field). This field must also be augmented by an effective anisotropy field H_A to account for the change in total anisotropy energy

[14] Joseph Callaway and D. C. McCollum, Phys. Rev. **130**, 1741 (1963).

[15] C. Herring and C. Kittel, Phys. Rev. **81**, 869 (1951).

[16] We are careful to label S_j differently than S_m because they represent different things. There is no way of defining S_j on a non-Heisenberg model. A separate assumptive value for S_j is of no interest in spite of the fact that it has been popular to quote values for J alone for materials in a manner based on the whim of the worker.

[17] S. H. Charap, Phys. Rev. **119**, 1538 (1960). These series are expansions of the Bose-Einstein integrals which were calculated by J. E. Robinson, Phys. Rev. **83**, 678 (1951).

[18] T. Holstein and H. Primakoff, Phys. Rev. **58**, 1098 (1940).

per spin-wave excited. This is given by[19]

$$H_A=-\frac{10K_1}{M_0}[\alpha_1^2\alpha_2^2+\alpha_2^2\alpha_3^2+\alpha_3^2\alpha_1^2-\tfrac{1}{5}], \quad (8)$$

with K_1, the first cubic anisotropy constant and α_i the direction cosines of the magnetization with respect to the crystalline axes. Finally, it is necessary to take into account the magnetic interaction between the spin waves and the magnetization of the system. This spin-wave demagnetization is a classical effect dependent only on our picture of a spin-wave as a wave-like disturbance of the otherwise uniform magnetization and has been treated as such by Herring and Kittel.[20] The result is that the energy of the spin wave depends upon its direction of propagation θ_k with respect to the magnetization according to

$$[\epsilon_k+g\beta(H+H_A)]\{1+g\beta 4\pi M_0 \sin^2\theta_k/[\epsilon_k+g\beta(H+H_A)]\}^{1/2}.$$

In the present case we may, however, use a single gap for all the spin waves. For the bulk of the spin waves excited in the temperature intervals used here the magnetic interaction need be retained only to first order. This is the so-called large k approximation of Herring and Kittel[15] in which the entire effect of this interaction on the spin-wave energy is simply given by the added gap

$$g\beta 2\pi M_0 \sin^2\theta_k.$$

In calculating the spin-wave populations again it is only the first-order effect of the magnetic interaction which is retained. The result is that at these temperatures the spread of these added gaps is not great enough to cause significant variation in the population of spin-wave states as a function of θ_k and the average added gap

$$g\beta\tfrac{4}{3}\pi M_0$$

may be used for all the spin waves.[21] It is interesting to note that this is precisely the gap produced by the Lorentz field.

In summary, then, the theoretical energy gap is

$$\epsilon_g=g\beta[H+H_A+\tfrac{4}{3}\pi M_0], \quad (9)$$

and one object of this experiment is to determine whether in fact this expression is acceptable for characterizing the behavior of pyromagnetic data on Fe and Ni at low temperatures.

According to the collective electron theory, the magnetization varies with temperature because of redistribution of electrons among the one-electron states, i.e., the transfer of electrons between the up- and down-spin bands.[22] This theory distinguishes two important cases: (1) all up-spin states lie at least ΔE in energy below the Fermi level which gives

$$\frac{M_0-M(T)}{M_0}=A(T)\exp[-\Delta E/k_BT], \quad (10)$$

and (2) unfilled states occur in both up- and down-spin bands at $T=0°K$ which leads to

$$\frac{M_0-M(T)}{M_0}=ST^2. \quad (11)$$

Because the data reveal none of the exponential character of Eq. (10), only the T^2 term is included in the phenomenological Eq. (1). The coefficient S depends upon the details of the band shape, and reliable estimates of its magnitude are not available. Herring and Kittel[15] and, most recently, Edwards[23] have argued that superposition of collective electron and spin-wave effects should be expected for metals, as indicated by Eq. (1). Magnetic effects have been regarded as significant only in modifying the spin-wave terms; in the collective electron theory they enter in direct comparison with the molecular field and weakly perturb what we shall see is a barely detectable contribution to Eq. (1).

Thermally induced lattice expansion is expected to account for some of the observed behavior of the magnetization through variation of the magnetic moment per atom with lattice separation.[24] Experiments[25] on pressure dependence of M for both Fe and Ni at room temperature indicate that it may be reasonable to express $(M_0-M(T))/M_0$ as linearly proportional to total expansion $(l(T)-l_0)/l_0$ as in Eq. (1).

III. PROCEDURE OF DATA ANALYSIS

The complete equation for the magnetization is characterized by a profusion of independent parameters and low order of separation of the various powers of T. Thus, it is not possible to obtain coefficients by fitting each term separately to data confined to an appropriate temperature range; nor is it possible to perform least-squares fitting to the complete equation since the data accuracy is, of necessity, finite. Instead it was determined that the theoretically expected spin-wave terms were dominant and an effort was then made to select the best second-order terms to perfect the data fitting to Eq. (1). We further employ conditions of internal consistency to narrow the range of possibilities. That

[19] F. Keffer and T. Oguchi, Phys. Rev. **117**, 718 (1960).

[20] This problem was also treated by Holstein and Primakoff (see Ref. 14) on the basis of the Heisenberg model with equivalent results.

[21] In our previous work (see Ref. 8) on analysis of Ni data, this term, which contributes only $\frac{1}{3}$ of a degree in T_g, was neglected in comparison with other effects now known to be spurious.

[22] E. C. Stoner, Proc. Roy. Soc. (London) **A165**, 372 (1938).

[23] D. M. Edwards, Proc. Roy. Soc. (London) **269A**, 338 (1962).

[24] Variation of the "exchange integrals" J_l with lattice separation will perturb the spin-wave spectrum. For the magnetization these are higher order effects beyond the range of this experiment.

[25] E. Tatsumoto, H. Fugiwara, H. Tange, and Y. Kato, Phys. Rev. **128**, 2179 (1962).

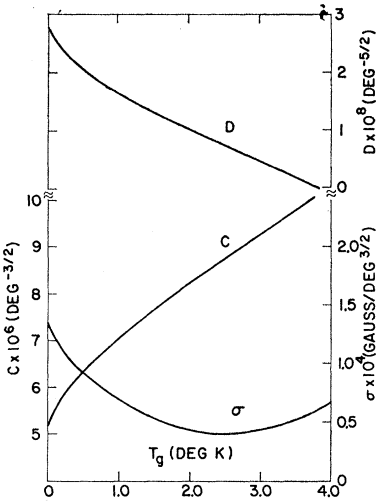

FIG. 4. Results of fitting to spin-wave theory data on the Ni crystal (see Fig. 1) up to 120°K with $H=6000$ Oe applied parallel to [111]. C and D were allowed to vary independently in the least-squares analysis while T_g was given a range of values from 0 to 4°K. Acceptable values of the parameters must fall within the broad minimum in the σ vs T_g plot. The theoretical gap temperature obtained from Eq. (9) is 1.5°K based on $g=2.19$, $H=6$ kOe, $M_0=508$ G and $K_1=-7.5\times10^5$ ergs/cc.

is, we require that the coefficients C and D be independent of the temperature and applied field. It will be seen that this requirement results in spin-wave parameters consistent with independent measurements of their energy.

A. Nickel

1. *Pure Spin-Wave Terms*

A least-squares fit of the full set of Ni data to spin-wave terms alone was first made over a range of assumed gap temperatures with C and D allowed to vary independently. Typical results are shown in Fig. 4 for data taken at an applied internal field of 6000 Oe. The observed minimum in standard deviation σ versus T_g falls near but slightly above the theoretical value for the effective energy gap 1.5°K given by Eq. (9).[26] Corresponding to the broadness in the minimum are ranges of acceptable values for C, D, and T_g and a correlation between them such that, if one can accept a known value for any one, the other two are determinable. Let us discuss the range of acceptable values in terms of an arbitrary upper limit for standard deviation chosen equal to 20% larger than the minimum. Under this condition Fig. 4 has T_g ranging from approximately the theoretical gap up to 1.7°K higher than the theoretical gap. At the same time, C adjusts itself upward by 20% from 7.5 to 9.5×10^{-6} deg$^{-3/2}$ and D extends from 1.4×10^{-8} deg$^{-5/2}$ down to nearly zero. Thus, it appears that an extra energy gap is required if D is known to be as close to zero as the nearest neighbor Heisenberg value ($\approx0.1\times10^{-8}$). On the other hand, if one believes in the theoretical value for the energy gap, then D takes on an extra large magnitude.

It is of fundamental interest to determine reliably which of these possibilities is correct.[27] To do this, we have imposed the internal consistency requirements that C is independent of T and H and that T_g varies with H according to Eq. (9).

The temperature dependence of C was tested by fitting to data from three ranges of temperature: 4.2 through 40, 70, and 120°K. When T_g was held fixed to values typified by the minimum in Fig. 4 (i.e., one degree larger than given by theory), the resulting values of C decreased with temperature. On the other hand, they were independent of temperature when T_g was fixed to agree with theory. The improvement can be characterized quantitatively: the standard deviation in the 12 values of C (obtained from the three tempera-

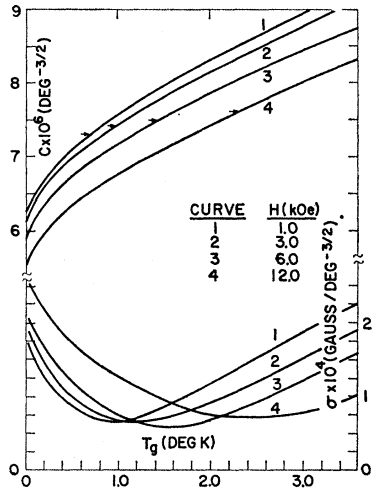

FIG. 5. Curves of σ versus T_g and C versus T_g obtained in fitting all data of Fig. 1 to the spin-wave equation. C was allowed to vary in the least-squares analysis while D was fixed to the self-consistent value 1.5×10^{-8} deg$^{-5/2}$ (see text). Arrows denote values of C that correspond to the theoretical value of T_g according to Eq. (9).

[26] The spread of energy gaps with θ_k as given by $\epsilon(k_\perp)-\epsilon(k_{||})=g\beta2\pi M_0$ is less than 0.5°K and consequently cannot account for the observed broadness in the σ versus T_g plot. The origin of this broadness has been studied using synthetic data calculated from spin-wave terms in which values of C, D, T_g, and M_0 that are typical of Ni had been injected. Random error typical of real data was introduced by rounding off the calculated synthetic data to the number of significant figures contained in the real data. The least-squares processing of this synthetic data essentially reproduced the broadness of Fig. 4. In addition, it was learned that by removing the $T^{5/2}$ effects from both the synthetic data and the fitting equation, the resulting $\sigma-T_g$ curve became considerably sharper. It is, therefore, indicated that data inaccuracy in conjunction with overlapping of effects of temperature terms differing from each other by factors of low order in T is the cause of uncertainty displayed by the analysis illustrated in Fig. 4.

[27] In our previous analysis of these data, a similar duality of possible interpretations was presented and we favored the small D-large T_g choice. The new analysis discussed in this paper is necessary because it has since been discovered that the evidence cited to support that choice was in error resulting from a mistake in the computer program used for the least-squares analysis. The corrected program used here has been subjected to rigid tests.

ture ranges for data at four applied fields) decreased from 12 to 3%, and that for the 12 fitted values of D dropped from ≈ 100 to 11%. The best average value for D is 1.5×10^{-8} or about 16 times the nearest neighbor Heisenberg (nnH) value. We choose to quote $\pm0.2\times10^{-8}$ as estimated accuracy based on the standard deviation of the 12 values of D.

To test whether T_g varies with H according to Eq. (9), it is useful in the least-squares analysis to fix D while scanning T_g and allowing C to vary. Fixing D reduces the interaction between overlapping terms which was responsible for the broadness of the σ versus T_g curve of Fig. 4. In Fig. 5 are curves of σ versus T_g and C versus T_g which resulted from holding D equal to 1.5×10^{-8} in the analysis of all data taken at four applied fields. Two effects are to be noted. The positions of the minima in σ versus T_g curves, which now are more readily defined, are observed to move consistently to higher values of T_g as H is increased. That these corresponding values of T_g are consistent with Eq. (9) and the known g-value[28] of 2.19 for Ni is demonstrated in Fig. 6 where the theoretical and experimental gaps are displayed. The theoretical effective energy gap given by Eq. (9) is represented by the solid line. To provide a scale of comparison the spread of energy gaps with direction of **k**-vector is given by the two dotted lines for **k** parallel and perpendicular to M. The intercepts are determined from $K_1=-7.5\times10^5$ ergs/cc and $M_0=508$ G, and the slope from $g=2.19$ for Ni. The second effect to be noted from Fig. 5 is that the values of C taken at the experimental gaps are 7.52, 7.55, 7.52 and 7.54×10^{-6}, a remarkably consistent set. Even with T_g fixed to the theoretical values, the corresponding set of C values (denoted by arrows) 7.32, 7.43, 7.49 and 7.62×10^{-6} show nearly the same consistency. The C values averaged over the two sets (7.53×10^{-6} and 7.47×10^{-6}) could have been made to coincide had a slightly larger fixed value for D been chosen. (The required increase would be comparable to the limit of accuracy in our determination of D.) We adopt an average of the two and conclude that $C=(7.5\pm0.2)\times10^{-6}$ is the best value for the results of a fit to pure spin-wave theory. The indicated accuracy is equal to the standard deviation from the average of C values obtained when D was allowed to vary with T_g equal to the theoretical value.

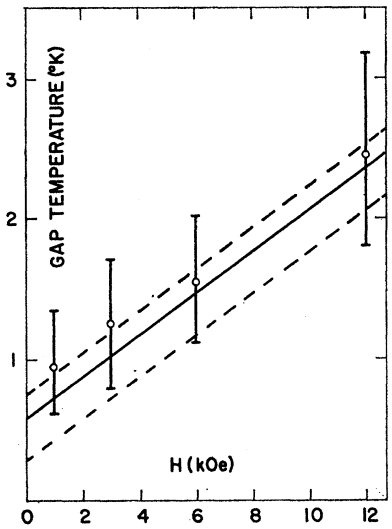

FIG. 6. Comparison of experimental and theoretical values for T_g in Ni as affected by an applied internal field H parallel to [111]. Circles are experimental points obtained from the minima in σ vs T_g curves of Fig. 5. Bars indicate accuracy as specified by an arbitrary limit on σ of 20% above its minimum. The solid line is given by Eq. (9) for the theoretical effective gap; whereas, the dotted lines are limits of the spread in T_g with θ_k caused by demagnetization energies of the spin waves. Known values of K_1 and M_0 specify the intercepts while $g=2.19$ determines the slope.

2. *Collective Electron Term*

A term in T^2 descriptive of collective electron theory cannot be the dominant term by virtue of the fact that magnetization data nearly fits to a fictitious T^n term with n between 1.7 and 1.8 depending on applied field.[29] Our only test is then to consider whether ST^2 replaces $DT^{5/2}$ in the role of a second dominant term. D was fixed equal to the small value 0.1×10^{-8} representative of a nearest neighbor only exchange interaction and T_g was set equal to the theoretical value for each of four fields. C and S were then allowed to vary in fitting data again over three temperature ranges. S took on the value $(1.9\pm0.2)\times10^{-7}$ as an average over twelve sets of data. The limits are the standard deviation of the twelve values from the average. The resulting values of standard deviation were about 5% larger on the average and the temperature dependence of C was three times larger than the results of fitting with S fixed to zero while C and D were allowed to vary. These results indicate that ST^2 is not a second dominant term when compared with the extra large $DT^{5/2}$ term found in part (1) above.

3. *Thermal Expansion Term*

Measurements of thermal expansion $\Delta l/l_0\Delta T$ on Ni by Nix and McNair[30] down to the temperature of liquid N_2 were shown by them to fit very well to a Grüneisen-Debye theory. The data they presented as a result of extending this theory to 4.2°K was used to establish the total linear expansion $[l(T)-l(4.2)]/l_0$ at one degree intervals for temperatures up to 120°K. It is readily shown that a term in the ΔM equation proportional to total expansion of the specimen cannot be a first dominant term. The total expansion varies much faster with the temperature than the magnetization-temperature

[28] A. J. P. Meyer and G. Asch, J. Appl. Phys. **32**, 330S (1961).

[29] That this exponent is noticeably greater than $\frac{3}{2}$ stems in part from the energy gap and the field dependence of n and can be accounted for by the modification of $CT^{3/2}$ by $\frac{1}{2}(\frac{3}{2},T/T_g)$. This point was demonstrated in Figs. 2 and 5 of Ref. 3.

[30] F. C. Nix and D. MacNair, Phys. Rev. **60**, 697 (1941).

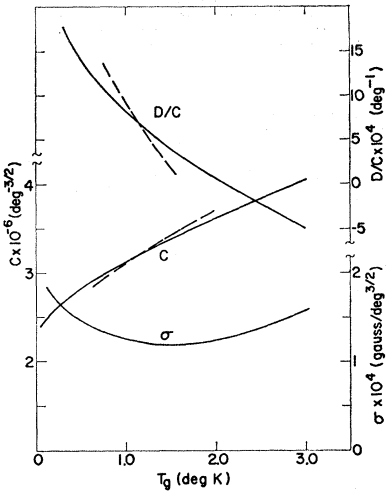

FIG. 7. Results of fitting data of Fig. 2 on Fe to spin-wave theory with C and D allowed to vary. Solid lines were obtained for data from 4–140°K and dotted lines represent the 4–90°K range. The theoretical effective gap temperature predicted by Eq. (9) is 2.05°K based on $g=2.09$, $H=6670$ Oe, $M_0=1752$ G and $K_1=+5.23\times10^5$ ergs/cc.

curves of Fig. 1. Stated otherwise, the slope of $[l(T)-l(0)]/l(0)$ versus temperature on a log-log scale is greater at every temperature and more temperature-dependent than the slope of a similar plot of magnetization data. Nevertheless, an admixture of this term with the dominant $T^{3/2}$ term might produce the required magnetization data behavior. A search for such a fit was made in the following way. T_g was fixed according to Eq. (9) and E, the coefficient of the thermal expansion term, was given several fixed values. For each value of E the computer calculated $E(\Delta l/l_0)$ from the table of $\Delta l/l_0$ stored in its memory and subtracted this from measured values of ΔM at each temperature. The resulting sets of data were then fitted to the remaining equation in closed form by the usual least-squares method. Curves of σ versus E obtained when D and S were fixed to zero produced minima at positive values of E ranging between 3 and 5 for different fields. This is, therefore, the amount of the thermal expansion term needed to replace the $T^{5/2}$ term from spin-wave theory. However, the magnitudes of σ were 50% larger than when D was allowed to vary and E was held fixed to zero. This poorer fit coupled with the fact that positive E would be inconsistent with the negative sign predicted by the pressure dependence of M^{25} implies that the thermal expansion does not replace the extra large $T^{5/2}$ term as the second dominant term. Curves of σ versus E obtained when D as well as C was allowed to vary showed a very broad minimum with a 10% improvement in σ at $E\approx-3$. Although this is of the right sign and about the right magnitude to agree with pressure experiments, the improvement is too small to be taken seriously.

B. Iron

1. *Spin-Wave Terms*

Magnetization data on the small iron sphere was fitted first to spin-wave terms alone in the temperature ranges 4–90° and 4–140°K. Allowing C and D to vary and scanning T_g yielded the curves in Fig. 7. The solid lines represent the full temperature range 4–140°K. The curve of σ versus T_g shows a very broad minimum centered near $T_g=1.5$°K in contrast to a theoretical 2.0°K predicted by Eq. (9) using $M_0=1752$ G, $H=6670$ Oe and $K_1=5.23\times10^5$ ergs/cc. An increase of 20% in σ above its minimum allows T_g to range from 0.5 to 2.7°K. Within this spread to T_g, C ranges from 2.8 to 3.9×10^{-6} while D/C ranges from 14 to -3×10^{-4}. The range of acceptable values of these parameters is considerably wider here than for the case of Ni. The decreased definition is caused by the decreased sphere size and its associated increase in error as shown in Fig. 3.

Results of processing the temperature range, 4–90°K, are given by the dotted lines in Fig. 7. The set of parameters that were the same for the two temperature ranges are given by the points of crossing between solid and dotted lines. It is remarkable that (1) both C and D satisfy consistency at the same energy gap, (2) the value of this energy gap (1.2°K) is indistinguishable from the theoretical value to our accuracy for this sample, and (3) as will be shown in Sec. IV, the value $C=3.25\times10^{-6}$ agrees very well with an independent experiment.

In order to insure that this set of parameters is not unique to these two temperature ranges, a third range of data (4–40°K) was examined. In this low-temperature region, the $T^{5/2}$ term has about the same magnitude as the data accuracy. Consequently, it is meaningless to allow it to vary in the least-squares fitting procedure. By fixing D to the best value according to the analysis

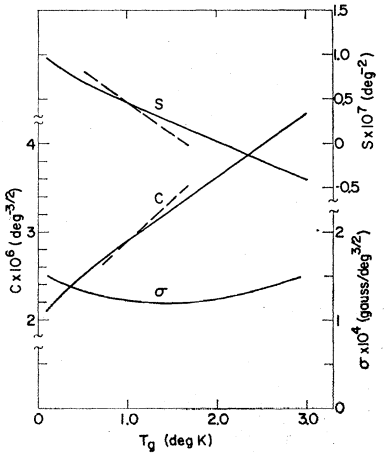

FIG. 8. Results of replacing the $T^{5/2}$ term in the spin-wave equation used for Fig. 7 by the collective electron term ST^2. C and S were allowed to vary while T_g was given several values from 0 to 3°K.

in Fig. 7, curves of C versus T_g (not shown) were obtained for all three temperature ranges. A crossing point common to all three curves occurred and was nearly identical to the one in Fig. 7 giving $C=3.28\times10^{-6}$ deg$^{-3/2}$ at $T_g=1.2$°K.

Although internal consistency has been accomplished for C and D at the same T_g, we note that its value 1.2°K is 0.8°K lower than given by Eq. (9). However, lack of sensitivity of the data to applied internal field over the available range ($\approx$7 kOe) implies an insensitivity to a corresponding expected change in T_g of 1.0°K. Thus, the observed discrepancy is not significantly different than theory and does not detract from the consistency analysis giving C and D. If one uses the effective gap of Eq. (9) (2.0°K), the value of C is only 10% larger (see Fig. 7).

2. *Collective Electron Term*

The term in ST^2 was treated as a second dominant term rather than a major term for the same reason spelled out in the analysis of nickel data in part A. Our only test is then to consider how well does ST^2 replace $DT^{5/2}$. Thus, D was fixed equal to zero and C and S were allowed to vary when T_g was set equal to several assumed values. Again 4–90° and 4–140°K data were processed to test for consistency. The results given in Fig. 8 show nearly the same features as the results in Fig. 7 where S was fixed to zero and D and C allowed to vary. The shape of the minimum in σ versus T_g for $D\equiv0$ (Fig. 8) is slightly more broad and the corresponding range of C is slightly larger than for the case $S\equiv0$ (Fig. 7). Even the position and magnitude of minimum are effectively identical for the two treatments. In no way was it possible from these and other tests to find evidence to argue that either ST^2 or $DT^{5/2}$ are more descriptive of higher order deviations from the major term in $T^{3/2}$.

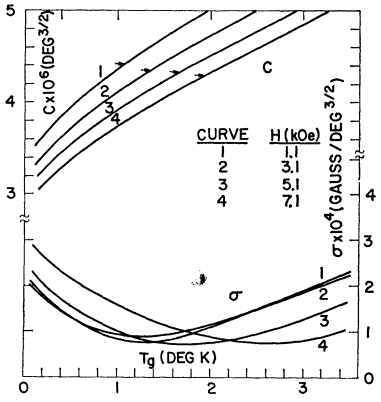

FIG. 9. Results of fitting to spin-wave theory the data from the Fe+3% Si (see Fig. 2) crystal measured up to 30°K at four internal fields H, applied parallel to the [110] crystal axis. The coefficient D of the $T^{5/2}$ term was held fixed to the best value obtained for the small pure iron crystal measured to higher temperatures. Arrows denote C values corresponding to the theoretical gap temperatures for each applied field H.

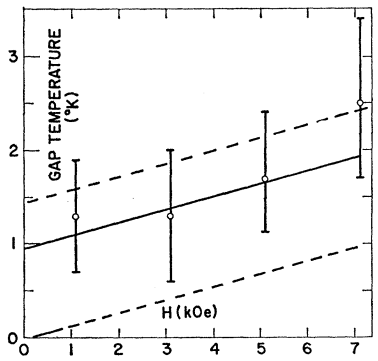

FIG. 10. Comparison of experimental and theoretical values of T_g for Fe+3% Si as affected by applied internal fields H. Circles are experimental points obtained from minima in curves of σ vs T_g in Fig. 9. Bars indicate accuracy as specified by arbitrary limit on σ of 20% above its minimum. The solid line is given by Eq. (9) for the theoretical effective gap; whereas the dotted lines are limits on the spread of T_g with θ_k caused by the demagnetization energies of spin waves. Known values of $K_1=432\times10^3$ ergs/cc and $M_0=1652$ G specify the intercept while $g=2.09$ determines the slope.

Since this distinction cannot be made, admixture of these two minor terms can equally well describe the data. Table I describes possible combinations in admixture. The results presented were obtained by fixing D to its best (5×nnH) and limiting values (0 and 10×nnH), fixing T_g to 1.0 and 1.2°K obtained from the consistency tests in Figs. 8 and 7 and allowing C and S to vary. The combined result can be summarized by saying that $C=(3.1\pm0.2)\times10^{-6}$ and $S\approx(0.1\pm0.3)\times10^{-7}$.

3. *Thermal Expansion Term*

A fit of magnetization data for Fe from Fig. 2 to a term in T^n gives a very nearly constant value of $n=1.62$ in the range 25 to 100°K whereas thermal expansion gives n varying from 3.0 at 100°K to 4.0 at 25°K. Because $\Delta l(T)/l_0$ varies so much faster with temperature than does the magnetization, it is easily seen that the term in $\Delta M/M_0$ proportional to total linear expansion cannot be the dominant term. Correspondingly, a study of the ability of the term $E\Delta l(T)/l_0$ to replace

TABLE I. Results of least-squares fit of Fe data up to 140° when C and S are allowed to vary. D was fixed to the best (5×nnH) and limiting values obtained in Fig. 7 while T_g was fixed to values satisfying internal consistency as shown in Figs. 7 and 8.

D_{fixed} (nnH)	T_g (°K)	$C\times10^6$ (deg$^{-3/2}$)	$S\times10^7$ (deg^{-2})	$\sigma\times10^4$ $\left(\frac{\text{G}}{\text{deg}^{3/2}}\right)$
0	1.0	2.91	0.45	1.21
	1.2	3.04	0.37	1.20
5	1.0	3.05	0.16	1.23
	1.2	3.19	0.08	1.20
10	1.0	3.20	−0.13	1.26
	1.2	3.34	−0.22	1.22

$DT^{5/2}$ or ST^2 as the second dominant term was made by fixing $D\equiv 0$, $S\equiv 0$ and $T_g\equiv 1.2$°K and finding the best value of E by the same procedure described for the case of nickel. This replacement found $E\approx 1$ as the fitted value, but σ was 5% larger and the sign of E disagrees with that predicted by the pressure dependence of the magnetization.[18] Analysis by fixing $E\equiv -1$, implied by the pressure experiments, and allowing D to vary, reduced σ by 5% and increased D to twice that resulting from the analysis of part $B1$ and Fig. 7. The improvement in fit is not enough to be significant but the change in D shows that the mere potential existence of like higher order terms can serve to modify a "best" value of the D coefficient.

C. Fe+3% Si Alloy

The low temperature, field-dependent deviations from the $T^{3/2}$ law are of primary consideration in this sample. Its extra volume, over that of the small pure iron sphere, enhances these effects but limits the temperature range as discussed in Sec. I. Consequently, investigation of high order deviations is omitted here. We fix the strength of the $T^{5/2}$ term to the apparent best result ($D\equiv 5\times$nnH) obtained in part B, while allowing C to vary and scanning T_g. (The contribution of this amount of the $T^{5/2}$ term to the total ΔM at the highest temperature (30°K) is little more than twice the data accuracy.) Results of this procedure are presented in Fig. 9 for data taken at four values of applied internal field. The positions of the minima in σ versus T_g correlate with the applied field and agree with theory as demonstrated in Fig. 10. The experimental points do not lie significantly outside of the theoretical limits on the spread of T_g with θ_k if we consider the limiting accuracy in T_g (shown as bars) to be given by the 20% increase in σ above its minimum value.

Having verified that the energy gaps obtained experimentally are consistent with theory, what is the value for C which can represent this alloy for any applied field? Corresponding to the theoretical gaps $T_g=1.10$, 1.38, 1.66 and 1.94°K for the four fields applied, we obtain $C=4.42$, 4.35, 4.33 and 4.30×10^{-6} from the curves of C versus T_g in Fig. 9. These values deviate by less than 2% from their average: $C=4.35\times 10^{-6}$. This then, provides a value which is independent of internal fields in the range (≈ 7 kOe) available. However, an uncertainty in C of the order of 5% is implied by the fluctuations in the measured gaps indicated in Fig. 10.

The difference between C values for Fe and Fe(Si) appears to be explained by considering the effect on the exchange parameter and on S_m of diluting pure iron with a non-magnetic impurity like silicon. These effects are considered quantitatively in Sec. IV.

IV. DISCUSSION OF RESULTS

Already indicated in part III are the range of values for the adjustable fitting parameters in the magnetization equation that produce an acceptable least-squares fit. For both Fe and Ni the term in $CT^{3/2}$ accounts for the dominant behavior of data over the major portion of the temperature range. Lower order field-dependent deviations from this term are explained by an energy gap in the spin-wave spectrum. Deviations of higher order for data on nickel are best accounted for by the $DT^{5/2}$ term, but for Fe the data provided no basis for choice between the $T^{5/2}$ and the collective electron term in T^2. The thermal expansion term, also investigated as a possible replacement for the $T^{5/2}$ term, is regarded as unsatisfactory in both materials.

The analysis of data on nickel produced well-defined results. The requirement from theory that C and D be independent of temperature and applied field was satisfied at very nearly the expected values of effective energy gap as predicted by the theoretical equation (9). The accuracy of agreement is best described by Figs. 5 and 6 and can be summarized by the statement that the experimental energy gaps increase with applied field at a rate that is consistent with $g=2.19$ in agreement with gyromagnetic measurements.[28] The corresponding best values of C and D for nickel are

$$C=(7.5\pm 0.2)\times 10^{-6}\ \text{deg}^{-3/2},$$
$$D=(1.5\pm 0.2)\times 10^{-8}\ \text{deg}^{-5/2},$$
$$D/C=2\times 10^{-3}\ \text{deg}^{-1}.$$

The C-coefficient is often used for characterizing the strength of the "exchange" interaction. It is popular for this purpose to replace $\sum_l J_l l^2$ in Eq. (4) and (5) by $6J\alpha_0^2$ which gives

$$C=\frac{2.612}{NS_m}\left(\frac{k_B}{8\pi S_j J\alpha_0^2}\right)^{3/2} \tag{12}$$

$$D=\frac{1.341}{NS_m}\frac{3\pi}{4}\left(\frac{k_B}{8\pi S_j J\alpha_0^2}\right)^{5/2}\left\{\frac{\sum_1 l^4 J_l}{J\alpha_0^2}\right\}. \tag{13}$$

The product JS_j rather than J alone is the parameter to be determined from the measured C as S_j is not known for a non-Heisenberg ferromagnet. A very satisfying result is that our value $JS_j=187\ k_B$ obtained through Eq. (12) from the above value for C for Ni is in excellent agreement with 195 k_B obtained independently by Lowde[5] measuring inelastic scattering of neutrons by spin waves. Spin-wave resonance measurements on thin films of Ni by Nose[31] yielded $JS_j=177\ k_B$ with a spread of $\pm 10\%$ in values obtained from five separate specimens.

The measured D/C is approximately sixteen times that predicted by a nearest neighbor Heisenberg model of exchange (nnH). This result can be interpreted through the fourth moment of the range of interaction in Eq. (13) as being indicative of an extra long range of interaction. An indication of this type has also been

[31] H. Nose, J. Phys. Soc. Japan **16**, 2475 (1961).

seen in neutron diffraction[5] and spin-wave resonance[32] experiments in the form of a $T^{5/2}$ dependence of the dispersion parameter[33] that is larger than that predicted from a simple nnH model. The mechanism of exchange interaction among spin waves which these experiments detect is entirely different than the origin of the $DT^{5/2}$ term and so quantitative comparison cannot be made unless they are connected by some ideal model. Making connection through the Heisenberg model with arbitrary range of interaction, we find the relation $N/D=\frac{4}{3}S_m/S_j$ between D and N. Here N is specified by the equation for the temperature dependence of the spin-wave energy due to exchange scattering between spin waves[33]

$$(JS_j)_T=(JS_j)_0[1-NT^{5/2}].$$

From our best value for D and the value $N=6.2\times10^{-8}$ inferred from neutron-diffraction data we have $N/D\simeq4.1$. Using this ratio and $S_m=0.27$, we obtain the result $S_j=0.09$ which is not consistent with the Heisenberg model upon which this calculation is based.

For the small crystal of pure iron, effects of applied field on the energy gap were not detectable within the available range of applied internal field, 7 kOe, which corresponds to an induced change in the energy gap of 1.0°K. Thus, it is not at all significant that the gap temperature at which consistency in C and D occurred was 0.8°K below the theoretical value. For sake of completeness we tabulate fitted values of C and D for the theoretical gap (second column) as well as the self-consistent values (first column).

	Pure Fe single crystal, $H_0=14$ kOe	
	$T_g=1.2$°K	$T_g=2.05$°K
$C(\text{deg}^{-3/2})$	3.25×10^{-6}	3.54×10^{-6}
$D(\text{deg}^{-5/2})$	2.1×10^{-9}	0
$D/C(\text{deg}^{-1})$	7×10^{-4}	0
$JS_j/k_B(\text{deg})$	209	197 based on $S_m=1.06$

Rodbell's ferromagnetic resonance experiment on single crystal whiskers[34] is probably the best independent determination of JS_j for iron. The same value for $S_m=(M_0/Ng\beta=1.06)$ used to convert C to JS_j for the table will convert Rodbell's exchange stiffness parameter $A(=(25\pm5)\times10^{-6}$ ergs/cm) to a value for $JS_j=(240\pm50)k_B$. Our two values listed above fall within these limits. The experimental ratios for D/C range between 0 and 5 times the nearest neighbor Heisenberg value. The uncertainty here becomes further enhanced by the fact that the collective electron term in ST^2 provides a good substitute for the $T^{5/2}$ term. Consideration of possible admixture of these two terms (Table I) has led us to establish limits for $D=5\pm5$ times nnH and $S\approx(0.1\pm0.3)\times10^{-7}$ deg^{-2}.

Effects of applied field on the energy gap in Fe are adequately represented by results from the larger crystal of Fe+3% Si. The gaps observed are consistent with theory as demonstrated in Figs. 9 and 10. A value for $C\approx4.35\times10^{-6}$ correlated well with T_g values taken from theory and can be used to specify $JS_j=178k_B$ for this alloy.

It is interesting to compare this with the C value (3.54×10^{-6}) for pure iron which was similarly correlated with the theoretical gap. That these are different is to be expected and we shall show that the observed 23% difference is plausible. Addition of nonmagnetic sites to the lattice may affect C in three ways. There is a reduction in the effective exchange (JS_j), in the total moment ($M_0\propto NS_m$) and in the total number of spin-wave states per unit volume. Because the exchange depends bilinearly on the spin per site (Heisenberg model) or spin density (Herring and Kittel model), one might expect a small fraction x of nonmagnetic sites to reduce JS_j by the factor $1-2x$. A more detailed argument yielding this result has been given by Keffer.[35] For the alloy Fe+3 wt %Si, $x\approx0.05$ and we expect a 10% reduction in JS_j from that for pure iron. This would account for 18% of the observed increase in C. The remaining 5% is adequately accounted for by the decrease (6%) in total moment from $M_0=1752$ to 1652 G. While it might be expected that the reduction in the total number of spin-wave states would also change C, for the long wavelength spin waves excited at these temperatures, the density of states should be proportional to the number of atomic rather than magnetic sites in the lattice. The atomic density changes by less than 0.5% and thus provides a negligible contribution to the change in C.

V. CONCLUSIONS

It is not out of place to emphasize once again the result of our experiment, namely, that the behavior of the magnetization of the cubic ferrometals, Ni and Fe, is very well described at low temperatures by the phenomenological spin-wave theory. Other mechanisms of magnetization change clearly play a minor role up to 15 or 20% of the Curie point. We have observed effects of applied fields on the curves of magnetization versus temperature which are well described by the inclusion of an energy gap in the spin-wave spectrum. Its magnitude is determined by applied internal field, anisotropy field and the average demagnetization energy of the spin waves. Thus, the pyromagnetic technique achieved indirectly a measurement of the low-temperature susceptibility of the intrinsic domain magnetization which had eluded workers for years. Fitted values of arbitrary parameters in the magnetization equation have provided some quantitative information about the shape of the spectrum of low spin-wave energies. Spe-

[32] P. E. Tannenwald, J. Phys. Soc. Japan **17**, Suppl. B-1, 592 (1962).
[33] F. Keffer and R. Loudon, J. Appl. Phys. **32**, 2S (1961).
[34] D. S. Rodbell, *Growth and Imperfections in Crystals* (John Wiley & Sons, Inc., New York, 1958), p. 247.
[35] F. Keffer, *Handbuch der Physik* (Springer-Verlag, Berlin, to be published).

cifically, the strength of the *quadratic* dependence on wave vector, which we infer for each metal, is essentially identical in magnitude with those obtained by independent experiments of a completely different nature.

At the same time, the term *quartic* in the wave vector is considerably greater than can be explained by coupling among only nearest-neighboring sites, at least for nickel. This result is in contrast with the Zener-Vonsovsky model of *s-d* exchange between the localized unfilled inner shell electrons and conduction electrons, for Kasuya[36] has shown that this model leads to a negative $T^{5/2}$ term with magnitude considerably smaller than is observed in this experiment. We have also seen that a comparison of our measured quartic dependence with inelastic neutron scattering results leads to inconsistency with the model of Heisenberg coupling with arbitrary range. This is not too surprising in view of the fact that recent calculations[37] of direct exchange yield exchange integrals which are too small and of the wrong sign. On the other hand, it has been shown[38] that the itinerant or collective electron model does exhibit spin waves in the transition metals when electron-electron interactions are included. A quantitative test of this model, such as we have presented for the Heisenberg and *s-d* exchange models, must await further development of the theory. It is hoped that our work will stimulate efforts in this direction.

ACKNOWLEDGMENT

The authors are indebted to J. W. Mitchell for his valuable assistance and to J. Reinke and W. J. Doherty for programing the least-squares analysis.

[36] T. Kasuya, Progr. Theoret. Phys. (Kyoto) **16**, 45 (1956).

[37] W. J. Carr, J. Phys. Soc. Japan **17**, Suppl. B-1, 36 (1962); R. E. Watson and A. J. Freeman, Phys. Rev. **124**, 1439 (1961).

[38] R. Kubo, T. Izuyama, D. Kim, and Y. Nagaoka, J. Phys. Soc. Japan **17**, Suppl. B-1, 67 (1962); M. M. Antonoff, Bull. Am. Phys. Soc. **8**, 227 (1963).

PHYSICAL REVIEW VOLUME 132, NUMBER 5 1 DECEMBER 1963

Reflectivity of Silver-Gold Alloys in the Spectral Region 1.8–5.0 eV

PAUL R. WESSEL
U. S. Naval Ordnance Laboratory, Silver Spring, Maryland
(Received 18 July 1963)

Experimental data for the absolute reflectivity of pure silver, pure gold, and Ag-Au alloys containing 5, 10, 20, and 50 at.% gold are presented for the spectral region 1.8–5.0 eV. Measurements were made on electropolished bulk samples and the results are discussed in terms of interband transitions. The effects of polishing and surface contamination on the reflectivity are also discussed. Sample preparation and polishing methods are described.

1. INTRODUCTION

THE optical properties of the noble metals have recently been studied in detail by several investigators.[1–5] In addition, the band structure underlying the optical properties has also been investigated.[2,6–8] From the results contained in Refs. 1–8 it seems reasonable to interpret the least energetic optical absorption in the noble metals as being due to an electron transition from the *d* band to levels near the Fermi surface.

This paper presents experimental data for the optical reflectivity of silver, gold, and silver-gold alloys in the energy range 1.8–5.0 eV. The experimental results are discussed in terms of the band structure and optical transitions. Some attention has been given to the problems of surface preparation and contamination and their effect on the reflectivity.

Section 2 describes the sample preparation, electrolytic polishing, and the apparatus employed in making the reflectivity measurements. Experimental results showing the effect of polishing and surface contamination on the reflectivity are given in Sec. 3. The reflectivity data are presented and discussed briefly in Sec. 4.

2. EXPERIMENTAL PROCEDURES

Slugs of the desired composition were obtained by melting silver and gold together in a fused silica crucible. The crucible was seated on a resistance heated tantalum strip in vacuum at a pressure of less than 10^{-4} Torr. Each slug was flattened on one face by hand lapping on standard metallographic silicon carbide papers. A mirror surface was then obtained by lapping on a metallographic polishing wheel with 6-μ and 1-μ diamond pastes.

The final surface was then produced by using a

[1] E. A. Taft and H. R. Philipp, Phys. Rev. **121**, 1100 (1961).
[2] H. Ehrenreich and H. R. Philipp, Phys. Rev. **128**, 1622 (1962).
[3] W. C. Walker, O. P. Rustgi, and G. L. Weissler, J. Opt. Soc. Am. **49**, 471 (1959).
[4] L. G. Schulz, Suppl. Phil. Mag. **6**, 102 (1957).
[5] S. Roberts, Phys. Rev. **118**, 1509 (1960).
[6] M. Suffczynski, Phys. Rev. **117**, 663 (1960).
[7] B. Segall, Phys. Rev. **125**, 109 (1962).
[8] J. A. Rayne, *The Fermi Surface*, edited by W. A. Harrison and M. B. Webb (John Wiley & Sons, Inc., New York, 1960), p. 266.